Cooperative diffusion of animals on the square lattice

1991 J. Phys. A: Math. Gen. 24 477

(http://iopscience.iop.org/0305-4470/24/2/020)

J. Phys. A: Math. Gen. 24 (1991) 477–492. Printed in the UK

Cooperative diffusion of animals on the square lattice

Jean-Christophe Toussaint, Jean-Marc Debierre and Loïc Turban

Laboratoire de Physique du Solide†, Université de Nancy I, BP 239, 54506 Vandoeuvre-lès-Nancy, France

Received 21 May 1990, in final form 22 October 1990

Abstract. The collective diffusion of N-particle lattice animals without vacancies and mass up to $N=86$ is investigated on the square lattice. Using the transfer matrix technique, a cluster fractal dimension $d_f = 1.5618 \pm 0.0012$ is found. The mean-square displacement of the centre of mass R^2 and the pair correlation function g_2 are determined by Monte Carlo simulations. This dynamical study gives the mass dependence of the diffusion coefficient $D \sim N^{-1.12 \pm 0.03}$ and the correlation function g_2 is shown to depend on many characteristic times τ_k. Scaling assumptions for R^2 and g_2 lead to the distinguishment of two characteristic times: τ which is the time necessary for the cluster to be translated by its radius of gyration R_g, and τ_2, the time necessary for a particle of the cluster to be moved approximately by R_g *inside* the cluster.

1. Introduction

Cooperative diffusion of polymer chains has been intensively investigated (Verdier and Stockmayer 1962) using lattice models and Monte Carlo algorithms with local deformations of the chain (for a recent review see Caracciolo and Sokal 1986). More recently, Kantor *et al* (1987) have examined the statics and the dynamics of tethered surfaces defined as two-dimensional manifolds (or 'sheet' polymers) embedded in a three-dimensional space. But very little has been done concerning the diffusion of lattice animals. Gould and Holl (1981) have studied a diffusion mechanism for an s-particle cluster, on a lattice whose sites are occupied (empty) with a probability p ($q = 1-p$). The diffusion mechanism consists in interchanging an arbitrary cluster particle and a near or distant empty surface site, with probability $q^{\Delta t}$, where Δt is the variation in the number of perimeter sites (Stauffer 1978). They have computed the diffusion coefficient of an isolated cluster in the three following limiting cases: $p \to 0$, lattice animals; $p = p_c$, percolation clusters; and $p \to 1$, compact clusters. A different approach where particle jumps are restricted to neighbouring positions was developed by van der Eerden *et al* (1977) to describe the diffusion of very small (less than 20 atoms) gold or silver clusters on plane alkali halide substrates. The pair interactions between two cluster atoms and between one atom and the substrate are taken into account and the evolution of the diffusion coefficient is studied as a function of temperature and cluster mass for small clusters. The diffusion of A clusters in an AB

† Unité de Recherche Associée au CNRS No. DO 155.

0305-4470/91/020477+16$03.50

alloy was investigated by Binder (1977) using a lattice gas model. In this case, due to evaporation and redeposition, the mass of the diffusing clusters may vary in time.

We introduce here a new model for the cooperative diffusion of an N-particle cluster on the square lattice. The particles undergo short-range jumps with the constraint that the cluster remains connected. Only the simplest version in which the particles interact as hard spheres is considered here.

The model is described in detail in section 2. The statics is analysed in section 3 using a phenomenological renormalization method. The definitions of the physical quantities of interest are given in section 4. The diffusion of the centre of mass of the cluster is studied in section 5 using a transfer matrix approach and a Monte Carlo algorithm. In section 6 we examine the diffusion of individual particles of the cluster in the centre of mass reference frame. Finally, scaling laws relating the static and dynamic exponents are derived in sections 7 and 8.

2. Description of the model

We consider an N-particle cluster on the square lattice for which two particles lying on first-neighbour sites are connected. In order to simulate a cooperative diffusion process, the particles of the cluster are moved to neighbouring empty sites. If we only allowed the jumps to first-neighbour sites, some configurations, e.g. a square cluster of four particles, could not diffuse. When we allow jumps to second-neighbour empty sites, this difficulty disappears and we get a diffusion process which is likely to be ergodic as discussed in section 5.1.

Since we want the N-particle cluster to remain connected, we have to examine the resulting configuration after each elementary jump. In order to avoid the inspection of the whole cluster, we forbid jumps breaking locally the cluster as well as those generating vacancies, i.e. those forming a closed loop of occupied sites surrounding unoccupied sites. Such clusters may be called lattice animals without vacancies and, up to seven particles, these clusters are equivalent to the usual lattice animals since no vacancy can be formed.

During the diffusion process, each particle, randomly selected with a frequency equal to $1/N$, attempts a jump to any one of its eight first- or second-neighbour sites (occupied or unoccupied) with equal probability, and the physical time is incremented by $1/N$.

For each particle, we define a local square centred on the particle and containing its eight first and second neighbours. Two particles in the same local square are connected when they are linked together by a set of first-neighbour particles belonging to the square. This definition of the connectivity spares computer time, since deciding whether a jump is allowed or not only requires the inspection of the local environment of the moving particle in its initial and final states. Two rules involving the local squares of the selected particle (figure 1) before and after its jump are necessary:

(i) in the initial local square, the diffusing particle must not form a vacancy and must remain connected to all the particles to which it was connected before the jump;

(ii) in the final local square, the diffusing particle must not connect together particles which were not connected before the jump.

This set of local connectivity rules ensures that the cluster remains connected, without vacancies, and the rules are reversible. In conclusion, only the jumps distorting locally the cluster surface are allowed.

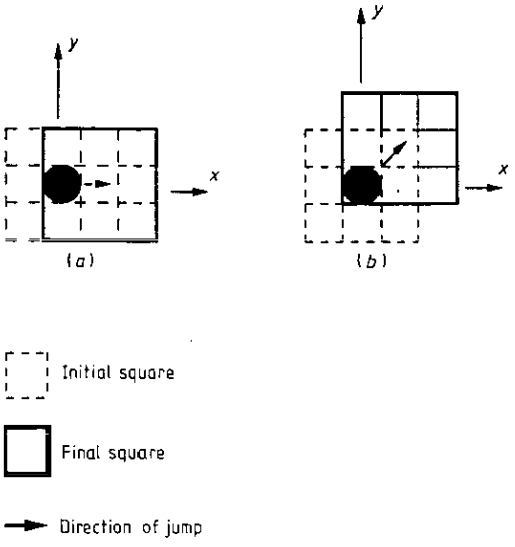

Figure 1. Local environment of a particle (black circle) on the square lattice for: (*a*) a jump to a first-neighbour empty site; (*b*) a jump to a second-neighbour empty site.

3. Static properties

In this section, the phenomenological renormalization approach (Nightingale 1976) is used to determine the static properties of lattice animals without vacancies on the square lattice. The method consists in calculating the correlation length ξ_n on a strip of width n, using a transfer matrix technique. We follow the procedure proposed by Derrida and De Seze (1982, hereafter referred to as DDS) for the lattice animal problem.

Let us consider the same example as in DDS in order to emphasize the differences between the two models. Using periodic boundary conditions on a strip of width $n=4$, we obtain the six configurations displayed in figure 2. In order to avoid an ambiguous definition for a vacancy on the strip, we have to modify slightly the definition of the connectivity given in DDS. In our case, the black sites in figure 2 are occupied and all connected together through a common root placed at column 0. For the same reason, we also have to eliminate the completely connected configuration (A) since, otherwise, virtual vacancies due to the periodic boundary conditions might appear as shown in figure 3.

As in DDS, we consider the correlation function $G_L(x)$ defined by

$$G_L(x)=\sum_N x^N \mathcal{N}_N(1, L) \tag{3.1}$$

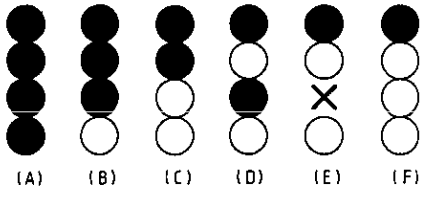

Figure 2. The six configurations on a strip of width $n=4$ with periodic boundary conditions. ●, occupied and connected site; ○, empty site; ×, occupied but not connected site.

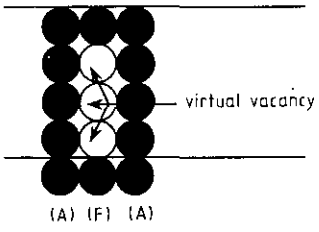

Figure 3. An example of virtual vacancies for a strip of width $n=4$. The last line is equivalent to the first one because of the periodic boundary conditions. ●, occupied and connected site; ○, empty site.

where $\mathcal{N}_N(1, L)$ is the number of animals of N sites connecting column 1 to column L. We may write

$$G_L(x) = B_L(x) + C_L(x) + D_L(x) + E_L(x) + F_L(x) = \sum_i \Omega_L^i(x) \tag{3.2}$$

where each term $\Omega_L^i(x)$ represents the part of the sum (3.1) over all animals spreading from column 1 to column L ending with the configuration Ω^i. The linear relations between the set of polynomials at column L and column $L+1$ are

$$\begin{aligned} B_{L+1} &= x^3(4B_L + 4C_L + 2D_L + 2E_L + 3F_L) \\ C_{L+1} &= x^2(4B_L + 3C_L + 4D_L + 2F_L) \\ D_{L+1} &= x^2(B_L + D_L) \\ E_{L+1} &= x^2(B_L + 2C_L + E_L + F_L) \\ F_{L+1} &= x(3B_L + 2C_L + 2D_L + F_L). \end{aligned} \tag{3.3}$$

These equations are very close to those found in DDS. The only difference is the third term of B_{L+1}: the factor 2 is the number of ways to connect configuration D at column L to configuration B at column $L+1$, the two remaining cases being forbidden because a vacancy is created (see figure 4).

Once the transfer matrix T is constructed,

$$\Omega_{L+1}^i = \sum_j T_{ij} \Omega_L^j \tag{3.4}$$

the leading eigenvalue $\lambda_n(x)$ is obtained by successive multiplications and the correlation length ξ_n is calculated as

$$\xi_n = -\frac{1}{\ln \lambda_n(x)}. \tag{3.5}$$

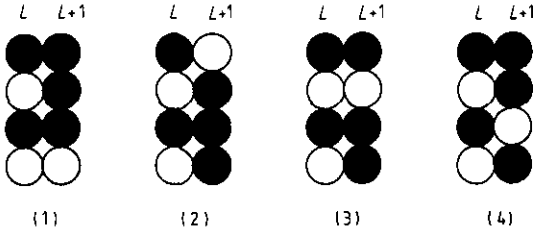

Figure 4. Different ways to go from configuration D at column L to configuration B at column $L+1$. The cases (1) and (3) are forbidden because a vacancy is formed. Symbols as in figure 3.

The critical fugacity x_c is determined by solving the fixed-point equation

$$\frac{\xi_n(x_c^{(n)})}{n} = \frac{\xi_{n-1}(x_c^{(n)})}{n-1}. \tag{3.6}$$

The critical exponent ν_n defined by $\xi_n \sim |x_c^{(n)} - x|^{-\nu_n}$ is finally given by

$$1 + \frac{1}{\nu_n} = \frac{\ln[(d\xi_n/dx)/(d\xi_{n-1}/dx)]}{\ln(n/n-1)} \tag{3.7}$$

where the derivatives are calculated at the fixed point $x_c^{(n)}$. For the largest strips, the critical exponent values ν_n and the fixed point values $x_c^{(n)}$ converge monotonically and can be extrapolated to $n = \infty$ (table 1). The sophisticated extrapolation method proposed by Derrida and Stauffer (1985) which gives $\nu = 0.64075 \pm 0.00015$ for usual lattice animals is not used here, since our largest strips are only nine-site wide. Our method consists instead in plotting the data versus $(n-1)^{-\alpha}$, were α is a parameter adjusted to give the best straight line on a log–log plot. For comparison, we tried the same method with our ν_n estimates and those found by Derrida and Stauffer (1985) for the same values of n. In figure 5, we observe that both series converge to $\nu = 0.6403 \pm 0.0005$,

Table 1. The fixed point $x_c^{(n)}$ and critical exponent ν_n estimates for strip width $3 \leqslant n \leqslant 9$. The extrapolated values are extracted from figures 3 and 4.

$n-1$	n	$x_c^{(n)}$	ν_n
2	3	0.198 95	0.5519 (1)
3	4	0.241 52	0.6348 (1)
4	5	0.243 41	0.6351 (1)
5	6	0.245 09	0.6374 (1)
6	7	0.245 84	0.6386 (1)
7	8	0.246 19	0.6392 (1)
8	9	0.246 39	0.6395 (1)
extrapolated		0.246 72 (3)	0.6403 (5)

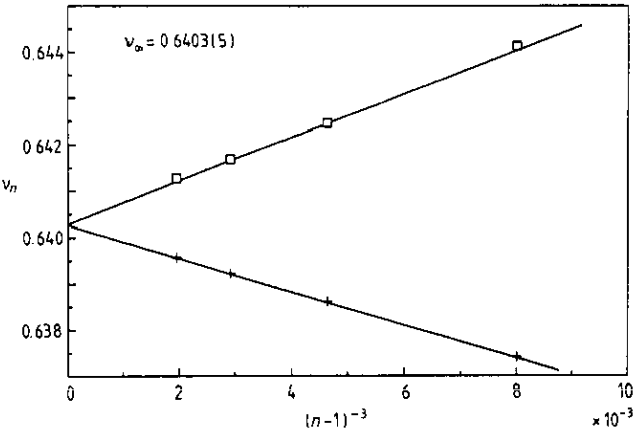

Figure 5. Plot of the critical exponent ν_n estimates against $(n-1)^{-3}$ for strips of width up to $n = 9$ (crosses). Also plotted are Derrida and Stauffer's (1985) results (dots) for lattice animals.

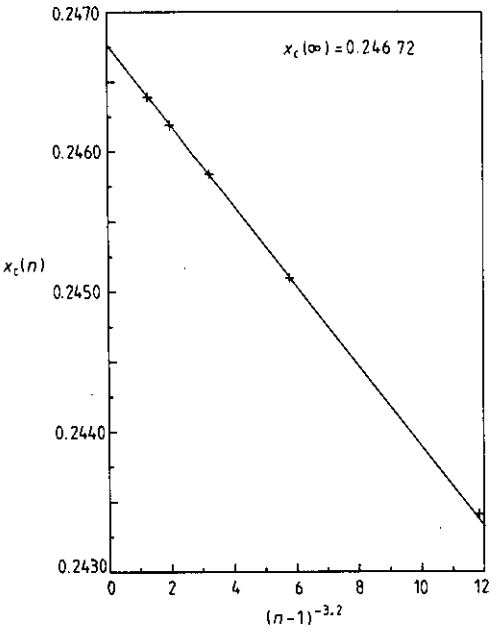

Figure 6. Plot of the fixed point values $x_c^{(n)}$ versus $(n-1)^{-3.2}$.

for the same value $\alpha = 3$ of the adjustable parameter. The critical exponent ν is probably the same in both cases, and the vacancies irrelevant. Finally, our estimate for the fixed point $x_c = 0.24672 \pm 0.00003$ (figure 6) is close but slightly higher than the value $x_c^0 = 0.24613 \pm 0.00001$ calculated by Derrida and Stauffer (1985). This is in agreement with an unpublished theorem by Madras (see also Whittington and Soteros 1990).

4. Definition of physical quantities

During the diffusion process, we calculate physical quantities related to the cluster shape (radius of gyration), the centre of mass motion (diffusion coefficient) and the diffusion of individual particles of the cluster (pair correlation function).

The radius of gyration gives an estimate of the geometrical extent of the cluster and is defined for an N-particle cluster as

$$\langle R_g^2 \rangle = \frac{1}{N^2} \sum_{i,j} \langle (\boldsymbol{r}_i - \boldsymbol{r}_j)^2 \rangle \tag{4.1}$$

where $\boldsymbol{r}_i(t)$ locates the position of the ith particle, at time t, in the laboratory reference frame. The angular bracket denotes a statistical average over all the cluster configurations. The initial position of the centre of mass is chosen as the origin,

$$\boldsymbol{R}(0) = \frac{1}{N} \sum_i \boldsymbol{r}_i(0) = 0 \tag{4.2}$$

so that the displacement of the centre of mass at time t,

$$\boldsymbol{R}(t) = \frac{1}{N} \sum_i \boldsymbol{r}_i(t) \tag{4.3}$$

leads to the mean-square displacement,

$$R^2(t) = \frac{1}{N^2} \sum_{i,j} \langle \boldsymbol{r}_i(t) \cdot \boldsymbol{r}_j(t) \rangle \tag{4.4}$$

related to the centre of mass diffusion coefficient,

$$D = \lim_{t \to \infty} \frac{R^2(t)}{4t}. \tag{4.5}$$

The correlation function for the relative position of a pair of particles i and j is defined as

$$g_2(N, t) = \frac{\Sigma_{j \neq i} \langle (\boldsymbol{r}_i(t) - \boldsymbol{r}_j(t))(\boldsymbol{r}_i(0) - \boldsymbol{r}_j(0)) \rangle}{\Sigma_{j \neq i} \langle (\boldsymbol{r}_i(0) - \boldsymbol{r}_j(0))^2 \rangle}. \tag{4.6}$$

5. Diffusion of the centre of mass

5.1. Dynamical transfer matrix method

The diffusion of the cluster may be studied by a transfer matrix method. As the number of cluster configurations increases rapidly with the mass N, this method is restricted to small sizes (up to six particles here) and it is necessary to use Monte Carlo calculations for larger clusters.

We use a dynamical transfer matrix whose elements T_{ji} give the probability after each jump attempt to find the cluster in configuration $|j\rangle$, if it was previously in configuration $|i\rangle$. As an example, the set of configurations explored by a cluster of mass $N = 3$ is given in figure 7. Let us calculate, for instance, the transition probability T_{61} from configuration $|1\rangle$ to configuration $|6\rangle$ (see figure 7). The transition may only be realized by moving the left-most particle of state $|1\rangle$ selected with a frequency $1/N = \frac{1}{3}$, along the south-east direction which is selected with a probability of $\frac{1}{8}$. The transfer matrix element for this jump is then

$$T_{61} = \langle 6|T|1\rangle = \frac{1}{8N}. \tag{5.1}$$

A useful property of the transfer matrix is

$$\sum_i T_{ji} = 1 \tag{5.2}$$

which simply states that the total probability to find the system in a given configuration $|j\rangle$, starting from all the possible initial configurations $|i\rangle$ is equal to one.

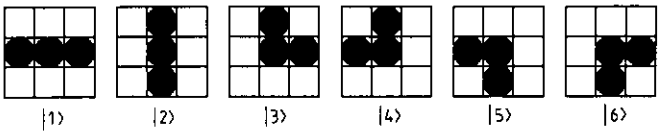

Figure 7. The six possible configurations for a cluster of mass $N = 3$.

An important question which arises now is the ergodicity of the model. Let $G_{fi}(t)$ be the probability of finding the system in a configuration $|f\rangle$ at time $t = n/N$, if it was in a configuration $|i\rangle$ at time $t = 0$:

$$G_{fi}(t) = \langle f|T^n|i\rangle. \tag{5.3}$$

The matrix T may be expressed in the basis of the transfer matrix eigenvectors $\{|\lambda_i\rangle\}$ associated to the eigenvalues λ_i:

$$T = \sum_i \lambda_i |\lambda_i\rangle\langle\lambda_i| \qquad \lambda_1 > \lambda_2 > \ldots > \lambda_k > \ldots. \tag{5.4}$$

Assuming that the largest eigenvalue λ_1 is non-degenerate, we obtain at large times:

$$G_{fi}(t) \to \lambda_1^n \langle f|\lambda_1\rangle\langle\lambda_1|i\rangle. \tag{5.5}$$

As $|\lambda_1\rangle$ is normalized, $|\langle i|\lambda_1\rangle|$ lies in the range [0, 1] and, when $\langle f|\lambda_1\rangle\langle\lambda_1|i\rangle$ is non-zero, $G_{fi} \to \infty$ for $\lambda_1 > 1$ whereas $G_{fi} \to 0$ for $\lambda_1 < 1$. Since

$$\sum_f G_{fi}(t) = 1 \tag{5.6}$$

λ_1 is necessarily equal to one, and from equation (5.2) it is easy to check that $|\lambda_1\rangle \sim (1 \ldots 1)^t$ is the corresponding eigenvector. The equilibrium distribution is therefore uniform and independent of the initial state of the system, so that the model is ergodic when λ_1 is non-degenerate. In practice, this has only been verified numerically for the smallest clusters $N \leq 6$.

We now examine the time evolution of the mean-square displacement $R^2(N, t)$ of the centre of mass of the cluster. Since the diffusion is isotropic, we only consider the motion of the centre of mass along the X-axis and, on average, we have $R^2(N, t) = X^2(N, t) + Y^2(N, t) = 2X^2(N, t)$. In order to calculate X^2, all the square centre of mass displacements $(\Delta X_{fi})^2$ from an initial state $|i\rangle$ to a final state $|f\rangle$ have to be weighted by the probabilities $G_{fi}(t)$ as follows:

$$X^2\left(t = \frac{n}{N}\right) = \sum_f (\Delta X_{fi})^2 G_{fi}(t). \tag{5.7}$$

To compute the elementary ΔX_{fi} for a transition from $|i\rangle$ to $|j\rangle$, we slightly modify the initial transfer matrix by multiplying each element T_{ji} by a factor $\exp(h\,\Delta X_{ji})$. The probability $G_{fi}(t)$ becomes a function of the field h and, using the asymptotic form of T^n for large times, relation (5.7) becomes

$$X^2\left(t = \frac{n}{N}\right) = \lim_{t\to\infty} \left\{\frac{\partial^2}{\partial h^2} \ln\left(\sum_f G_{fi}^{(n)}(h)\right)\right\}_{h=0} = Nt\left\{\frac{1}{\lambda_1}\frac{\partial^2 \lambda_1}{\partial h^2}\right\}_{h=0}. \tag{5.8}$$

The diffusion coefficient of the centre of mass is then defined by

$$D = \frac{X^2(t = n/N)}{2t} = \frac{N}{2}\left\{\frac{1}{\lambda_1}\frac{\partial^2 \lambda_1}{\partial h^2}\right\}_{h=0}. \tag{5.9}$$

The data for the diffusion coefficient $D(N)$ are given in table 2, together with those for larger systems obtained by Monte Carlo simulations.

Table 2. The diffusion coefficient D obtained by the transfer matrix method for $N \leq 6$ and by the Monte Carlo algorithm for clusters containing up to $N = 86$ particles.

N	D (Transfer matrix)	D (Monte Carlo)
2	0.062 50	—
3	0.027 78	0.0274 ± 0.0009
4	0.017 76	0.0184 ± 0.0004
5	0.012 83	0.0127 ± 0.0004
6	0.010 02	0.0100 ± 0.0003
7	—	$8.29 \times 10^{-3} \pm 0.24 \times 10^{-3}$
8	—	$6.91 \times 10^{-3} \pm 0.22 \times 10^{-3}$
11	—	$4.63 \times 10^{-3} \pm 0.16 \times 10^{-3}$
16	—	$2.98 \times 10^{-3} \pm 0.21 \times 10^{-3}$
20	—	$2.27 \times 10^{-3} \pm 0.04 \times 10^{-3}$
26	—	$1.64 \times 10^{-3} \pm 0.05 \times 10^{-3}$
38	—	$1.09 \times 10^{-3} \pm 0.04 \times 10^{-3}$
47	—	$8.49 \times 10^{-4} \pm 0.27 \times 10^{-4}$
58	—	$6.87 \times 10^{-4} \pm 0.25 \times 10^{-4}$
86	—	$4.51 \times 10^{-4} \pm 0.20 \times 10^{-4}$

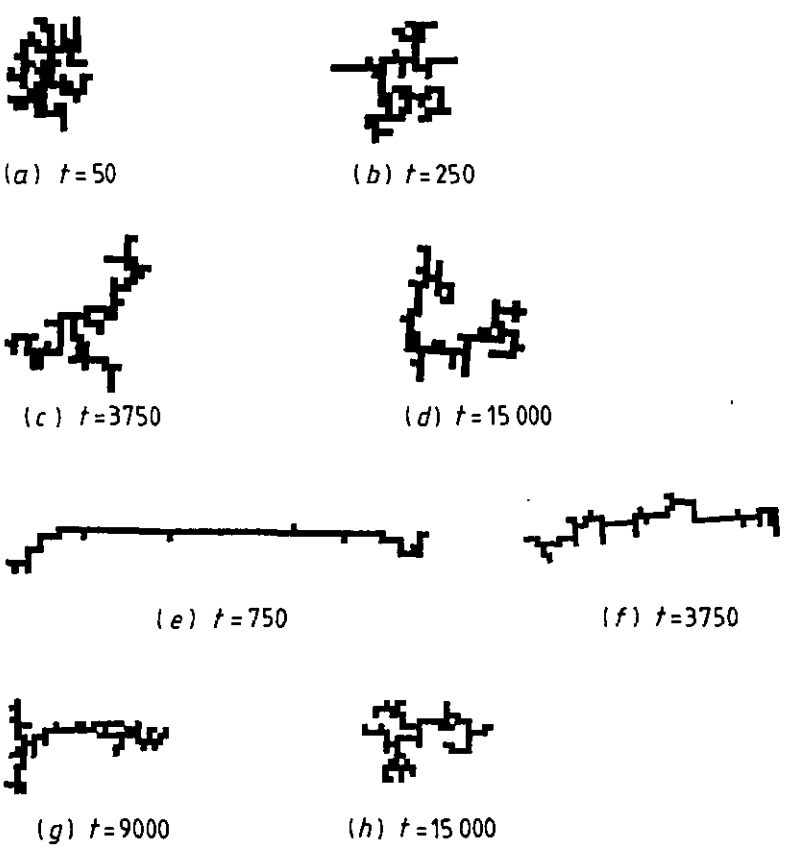

Figure 8. Evolution towards equilibrium of a cluster containing 86 particles. Four typical steps have been represented, when starting from a square configuration ((*a*) to (*d*)) and a linear configuration ((*e*) to (*f*)).

5.2. Monte Carlo algorithm

We briefly describe the Monte Carlo algorithm used to study the properties of larger clusters containing up to $N = 86$ particles. At each Monte Carlo step:

(i) a particle is randomly selected and the physical time is incremented by $1/N$;

(ii) a site among the eight first and second neighbours of the particle is chosen at random;

(iii) the jump is allowed if this site is empty and if the two local rules defined in section 2 are respected.

In the first part of a simulation the system evolves towards equilibrium (figure 8) which is assumed to be reached when two different initial configurations (square and linear) lead to the same radius of gyration. The physical quantities of interest are then computed and averaged over a large number of independent runs.

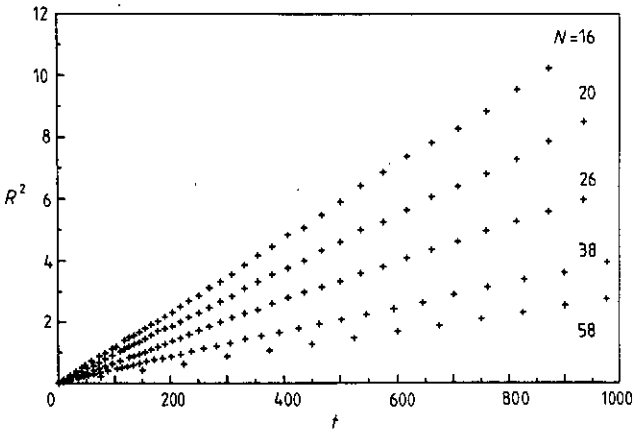

Figure 9. The time evolution of the mean-square displacement of the centre of mass, for clusters containing N particles ($16 \leq N \leq 58$). The diffusion coefficient decreases when the mass increases.

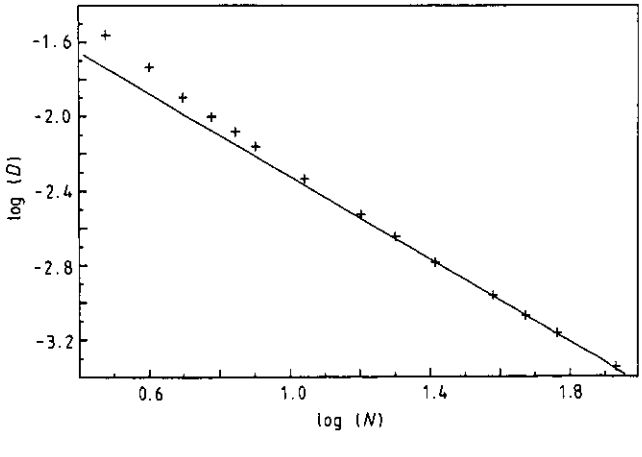

Figure 10. Plot of $\log(D)$ against $\log(N)$. A linear fit for the large N gives the estimate $u = -1.12 \pm 0.03$.

5.3. Mean-square centre of mass displacement

The mean-square displacement $R^2(N, t)$ of the cluster centre of mass is computed as a function of time t and mass N. We observe a Gaussian diffusion law $R^2 \sim Dt$, for all the cluster sizes (figure 9), and the diffusion coefficient D given by the slope of the curves decreases when N increases. The data (see table 2) are consistent with a power law

$$D \sim N^u. \tag{5.10}$$

Also given in table 2 are the D-values obtained by the transfer matrix method for $N \leq 6$ (see section 5.1) providing a check of the Monte Carlo data for small sizes. In figure 10, we plot $\log(D)$ versus $\log(N)$ for the largest clusters. The curve follows a straight line whose slope gives the estimate $u = -1.12 \pm 0.03$, a value slightly lower than $u = -1$ obtained for the polymer chains (Verdier and Stockmayer 1962).

6. Pair correlations inside the cluster

The diffusion of the individual particles of the cluster which is at the origin of the collective motion is also investigated. For this purpose, we compute the pair correlation function $g_2(N, t)$ which is simply related to the mean square particle displacement in the centre of mass reference frame:

$$r^2(N, t) = \frac{1}{N} \sum_i \langle (\boldsymbol{r}_i(t) - \boldsymbol{R}(t) - \boldsymbol{r}_i(0))^2 \rangle. \tag{6.1}$$

In order to prove this assertion, we develop the numerator in (4.6) and use (4.2) to get

$$g_2(N, t) = \frac{2}{NR_g^2} \sum_i \langle \boldsymbol{r}_i(t) \cdot \boldsymbol{r}_i(0) \rangle \tag{6.2}$$

so that, using (4.2) once more,

$$g_2(N, t) = \frac{2}{NR_g^2} \sum_i \langle \boldsymbol{r}_i(0) \cdot (\boldsymbol{r}_i(t) - \boldsymbol{R}(t)) \rangle. \tag{6.3}$$

Using the same approach for R_g^2 in the initial equilibrium state and at time t, we obtain

$$R_g^2 = \frac{2}{N} \sum_i \langle \boldsymbol{r}_i^2(0) \rangle = \frac{2}{N} \sum_i \langle (\boldsymbol{r}_i(t) - \boldsymbol{R}(t))^2 \rangle. \tag{6.4}$$

The last two equations give the different terms appearing when the square in (6.1) is developed and, altogether, we have

$$r^2(N, t) = R_g^2(1 - g_2(N, t)). \tag{6.5}$$

As shown in the appendix, the pair correlation function depends on many characteristic times τ_k:

$$g_2(N, t) = \sum_k A_k \, e^{-t/\tau_k} \tag{6.6}$$

with $\Sigma_k A_k = 1$ and $\tau_2 > \tau_3 > \tau_4 \ldots$. At large times, only the largest characteristic time τ_2 remains and $g_2(N, t)$ is given by

$$g_2(N, t) = A_2 \, e^{-t/\tau_2}. \tag{6.7}$$

To determine the amplitudes A_k and the characteristic times τ_k appearing in g_2, we use the following recursive method:

(i) A_2 and τ_2 are obtained by a linear fit of $\ln(g_2(N, t))$ against $\ln(t)$, for large times.

(ii) The difference $g_2(N, t) - A_2 \exp(-t/\tau_2)$ is then calculated and the same method as above is repeated to get A_3 and τ_3, and so on.

For a cluster of mass $N = 47$, only the three first terms of $g_2(N, t)$ can be calculated using our Monte Carlo data, and we get

$$\begin{aligned} A_2 &= 0.79 \qquad A_3 = 0.15 \qquad A_4 = 0.06 \\ \tau_2 &= 938 \qquad \tau_3 = 291 \qquad \tau_4 = 58. \end{aligned} \tag{6.8}$$

The main difficulty of this method is the loss of accuracy at each iteration which prevents reliable estimates to be made for high-order terms. For this reason, we only use the largest characteristic time τ_2 which, as can be seen in table 3, increases with the mass N. Plotting $\log(\tau_2)$ versus $\log(N)$ (figure 11) for the largest clusters ($16 \leqslant N \leqslant 86$), we obtain a straight line, so that

$$\tau_2 \sim N^p$$

with $p = 1.8 \pm 0.1$. According to equation (6.5), τ_2 is the time needed for a particle to be moved by R_g in the centre of mass reference frame.

Table 3. τ_2 values obtained by the Monte Carlo algorithm for clusters containing up to $N = 86$ particles.

N	τ_2
26	331
38	630
47	934
58	1377
86	2520

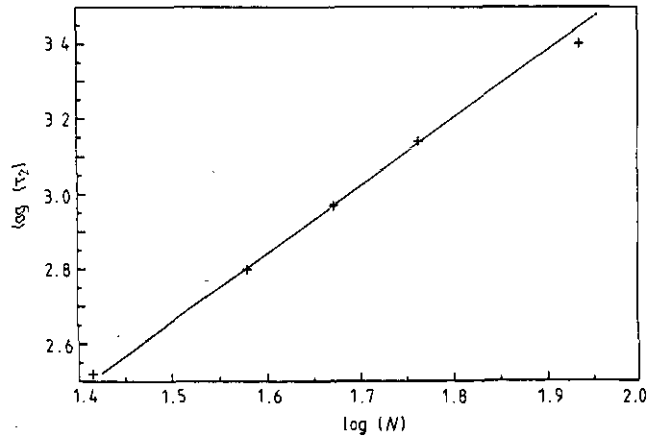

Figure 11. Plot of $\log(\tau_2)$ against $\log(N)$. A linear fit gives $-y_1'/d_1 = 1.8 \pm 0.1$.

7. Scaling for the mean-square centre of mass displacement

Assuming that $R^2(N, t)$ is a homogeneous function of N and t,

$$R^2(N, t) = b^2 R^2(b^{-d_f} N, b^{y_t} t) \tag{7.1}$$

with $b = t^{-1/y_t}$, one gets

$$R^2(N, t) = t^{-2/y_t} f\left(\frac{t}{\tau}\right) \tag{7.2}$$

where $\tau \sim N^{-y_t/d_f}$ is a characteristic time for the diffusion of the centre of mass. At large times, the scaling function $f(x)$ decreases as a power law,

$$f(x) \sim x^{\omega} \qquad \text{with } x = t/\tau \tag{7.3}$$

and relation (7.2) becomes

$$R^2(N, t) = t^{-2/y_t + \omega} N^{\omega y_t/d_f}. \tag{7.4}$$

Since the centre of mass diffusion is Gaussian

$$R^2(N, t) \sim Dt \sim N^u t \tag{7.5}$$

and the last two relations lead to the scaling laws

$$y_t = ud_f - 2 \tag{7.6}$$

$$\omega = \frac{ud_f}{y_t}. \tag{7.7}$$

With the previous estimates of $d_f = 1/\nu = 1.5618 \pm 0.0012$ and $u = -1.12 \pm 0.03$, one gets

$$y_t = -3.75 \pm 0.05 \qquad \text{and} \qquad \omega = 0.47 \pm 0.04. \tag{7.8}$$

The scaling assumption (equation 7.2) and the asymptotic behaviour of $f(x)$ are numerically tested by plotting $\log(R^2/t^{-2/y_t})$ versus $\log(t/N^{-y_t/d_f})$, for different N-values in the range $N = 8$-86 (figure 12). All the data are satisfactorily gathered along a straight line and a simple linear fit gives the slope $\omega = 0.47 \pm 0.09$ in excellent agreement with the above value (equation 7.8).

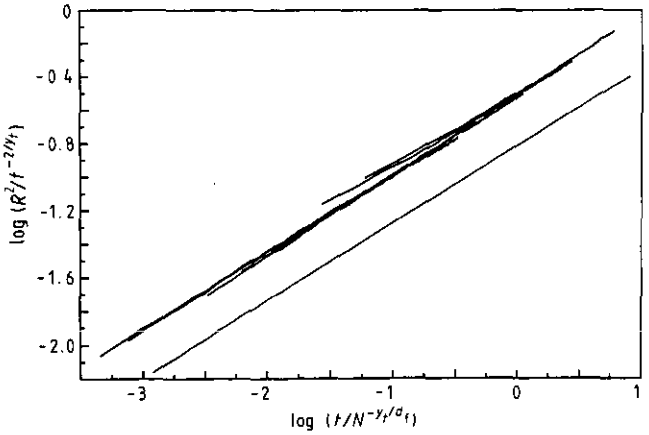

Figure 12. Plot of $\log(R^2/t^{-2/y_t})$ against $\log(t/N^{-y_t/d_f})$ for cluster masses in the range $N = 8$-86. A straight line is obtained with a slope $\omega = 0.47 \pm 0.09$.

Using relations (7.2) and (7.6), one gets

$$\tau \sim N^{-y_t/d_f} \sim N^{-(ud_f-2)/d_f} \sim N^{-u}N^{2/d_f} \sim D^{-1}R_g^2 \tag{7.9}$$

so that τ is the time necessary for a root-mean-square displacement of the centre of mass by R_g.

8. Scaling for the pair correlations inside the cluster

We assume that the pair correlation function $g_2(N, t)$ is a homogeneous function of N and t, so that

$$g_2(b^{-d_f}N, b^{y_t'}t) = b^0 g_2(N, t) \tag{8.1}$$

where a new exponent y_t' associated to the particle diffusion, different from y_t, has been introduced. For a scaling factor $b \sim N^{1/d_f}$, we obtain

$$g_2(N, t) = h(t/N^{-y_t'/d_f}) = h\left(\frac{t}{\tau_2}\right) = h(x) \tag{8.2}$$

where $\tau_2 \sim N^{-y_t'/d_f}$ and $x = t/\tau_2$. Since $\tau_2 \sim N^p$ (equation (5.9)), $p = -y_t'/d_f$ and, finally,

$$y_t' = -2.8 \pm 0.2. \tag{8.3}$$

In order to check the scaling assumption for $g_2(N, t)$ at large times, we plot the function $h(x)$ versus x (figure 13). Since $g_2(N, t)$ depends on several characteristic times, the scaling observed at small times ($x < 1$) is somewhat fortuitous.

As the centre of mass diffusion is due to the cooperative motion of the cluster particles, the two characteristic times $\tau \sim N^{-y_t/d_f}$ and $\tau_2 \sim N^{-y_t'/d_f}$ must be related in some way. We propose the following empirical relation:

$$y_t' = y_t + 1 \tag{8.4}$$

which is well verified by our numerical results ($y_t' = -2.8 \pm 0.2$ and $y_t = -3.75 \pm 0.05$) as well as for other cooperative diffusion models in one, two and three dimensions which are currently being studied and for which results will be published later.

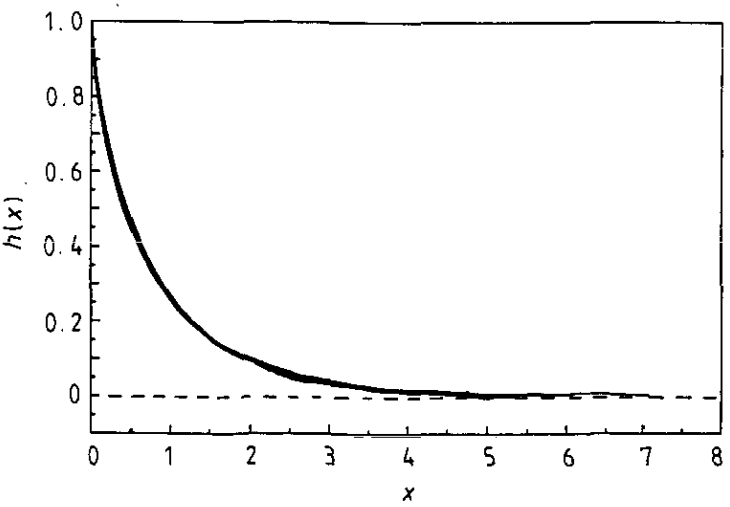

Figure 13. Plot of $h(x)$ against x as a check of the scaling assumption for $g_2(N, t)$ at large times. All the curves gather together along a unique one.

Appendix. Properties of the pair correlation function

In order to compute $g_2(N, t)$, one may use another transfer matrix T' which is much larger than the matrix T used to calculate $R^2(N, t)$ in section 5.1. Since we have now to distinguish the particles, the number of configurations increases very rapidly with the cluster mass N and this method cannot be used in practice. However, it is a useful tool for a better understanding of the correlations inside the cluster. A relation similar to 5.2 may be written for the probability conservation and the leading eigenvalue of T' is also $\lambda_1' = 1$, with the eigenvector

$$|\lambda_1'\rangle \sim (1, 1 \ldots 1)' \sim \sum_{\Omega} |\Omega\rangle \tag{A1}$$

where $|\Omega\rangle$ is a state associated to a cluster configuration with distinguishable particles.

We introduce here a diagonal vectorial operator $\hat{\boldsymbol{r}}_{ij}$ in the basis of the cluster configurations $|\Omega\rangle$ whose eigenvalues $\boldsymbol{r}_{ij} = \boldsymbol{r}_i - \boldsymbol{r}_j$ are simply the vectors joining the positions of the particle pairs (i, j):

$$\hat{\boldsymbol{r}}_{ij}|\Omega\rangle = \boldsymbol{r}_{ij}|\Omega\rangle. \tag{A2}$$

Starting from the equilibrium state $|\lambda_1'\rangle$, the pair correlation function at time t is obtained by summing over the whole set of configurations,

$$g_2\left(t = \frac{n}{N}\right) = \frac{\Sigma_\Omega \Sigma_{i,j} \langle \Omega | \hat{\boldsymbol{r}}_{ij} \hat{T}'^n \hat{\boldsymbol{r}}_{ij} | \lambda_1' \rangle}{\Sigma_\Omega \Sigma_{i,j} \langle \Omega | \hat{\boldsymbol{r}}_{ij}^2 | \lambda_1' \rangle} \tag{A3}$$

or, with (A1),

$$g_2\left(t = \frac{n}{N}\right) = \frac{\Sigma_{i,j} \langle \lambda_1' | \hat{\boldsymbol{r}}_{ij} \hat{T}'^n \hat{\boldsymbol{r}}_{ij} | \lambda_1' \rangle}{\Sigma_{i,j} \langle \lambda_1' | \hat{\boldsymbol{r}}_{ij}^2 | \lambda_1' \rangle} \tag{A4}$$

which, using the complete set of eigenvectors $\{|\lambda_k'\rangle\}$ of the T' matrix, becomes

$$g_2\left(t = \frac{n}{N}\right) = \frac{\Sigma_{k \neq 1} \Sigma_{i,j} \lambda_k'^n |\langle \lambda_k' | \hat{\boldsymbol{r}}_{ij} | \lambda_1' \rangle|^2}{\Sigma_{k \neq 1} \Sigma_{i,j} |\langle \lambda_k' | \hat{\boldsymbol{r}}_{ij} | \lambda_1' \rangle|^2} \tag{A5}$$

where $\lambda_1' > \lambda_2' > \ldots > \lambda_k' > \ldots$. The leading eigenvalue λ_1' does not appear in the g_2 expression since the element $\langle \lambda_1' | \hat{\boldsymbol{r}}_{ij} | \lambda_1' \rangle$ corresponding to the average $\langle \boldsymbol{r}_{ij} \rangle$ over all the vector orientations vanishes.

In summary, the pair correlation function depends on many characteristic times $\tau_k = -1/\ln \lambda_k'$ such as

$$g_2(N, t) = \sum_k A_k \, \mathrm{e}^{-t/\tau_k} \tag{A6}$$

with $\Sigma_k A_k = 1$, $\tau_{k+1} < \tau_k$ and $\tau_2 = \max\{\tau_k\}$.

References

Binder K 1977 *Phys. Rev.* B **15** 4425
Caracciolo S and Sokal A D 1986 *J. Phys. A: Math. Gen.* **19** L797
Derrida B and De Seze L 1982 *J. Physique* **43** 475
Derrida B and Stauffer D 1985 *J. Physique* **46** 1623
Gould H and Holl K 1981 *J. Phys. A: Math. Gen.* **14** L443
Kantor Y, Kardar M and Nelson D R 1987 *Phys. Rev.* A **35** 3056

Madras N unpublished
Nightingale M P 1976 *Physica* **83A** 561
Stauffer D 1978 *Phys. Rev. Lett.* **41** 1333
van der Eerden J P, Kashchiev D and Bennema P 1977 *J. Crystal Growth* **42** 31
Verdier P H and Stockmayer W H 1962 *J. Chem. Phys.* **36** 227
Whittington S G and Soteros C E 1990 *Disorder in Physical Systems* ed G Grimmett and D Welsh (Oxford: Oxford University Press)